

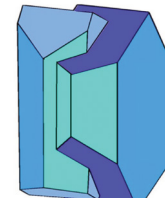
# Book of Tutorials and Abstracts



European  
Microbeam Analysis Society



University of  
BRISTOL



**EMAS 2018**

**13th EMAS Regional Workshop**

**MICROBEAM ANALYSIS IN THE EARTH SCIENCES**

**4 - 7 September 2018**

University of Bristol, Wills Hall, Bristol, Great Britain

---

Organised in collaboration with:  
Mineralogical Society of Great Britain and Ireland  
and  
University of Bristol

---



## TRACE ELEMENT ANALYSIS OF EXTRATERRESTRIAL OLIVINE

T. Gregory<sup>1,2</sup>

- 1 University of Bristol, School of Earth Sciences, Bristol Isotope Group  
Wills Memorial Building, Queens Road, Bristol BS8 1RJ, Great Britain
- 2 Natural History Museum, Department of Earth Sciences  
Cromwell Road, SW7 5BD, London, Great Britain  
e-mail: timothy.gregory@bristol.ac.uk

Tim Gregory discovered cosmochemistry during an undergraduate internship at NASA's Johnson Space Center (Houston, Texas) in 2014, as part of the Lunar and Planetary Institute Summer Internship. During this internship, he had his first taste of using scanning electron microscopy (SEM) and electron probe microanalysis (EPMA) to investigate the fine-scale lithological make-up of the oldest and most primitive rocks in the Solar System: chondrites. In the final year of his MEarthSci degree in Geology with Planetary Science at the University of Manchester, he extensively used SEM and EPMA in his MEarthSci project, where he was researching the geological history of a class of basaltic meteorites called howardites. Upon finishing his MEarthSci degree in 2015, Tim began his adventures in the world of isotope cosmochemistry in his PhD at the University of Bristol. While the focus of Tim's PhD is measuring the Mg-isotopic composition of meteorites to high precision, he extensively characterises the petrology and major- and minor-element composition of his samples prior to any destructive isotope analyses. This involves imaging in both backscattered electrons and energy-dispersive X-ray spectroscopy using an SEM, and careful chemical characterisation using EPMA.

## 1. INTRODUCTION

Chondrites are a type of meteorite that never melted on the asteroids from which they originate. The mm- to  $\mu\text{m}$ -sized inclusions from which they are made have therefore remained almost completely unchanged since they formed in the protoplanetary disk, making them ideal targets for the study of early Solar System processes.

While chondrites never melted, most did undergo post-accretion modification on their parent asteroids. To describe this change, a chondrite is assigned a petrologic type (Fig. 1). Type 3 through 6 indicate an increasing degree of equilibration (thermal metamorphism), and type 2 through 1 indicate an increasing degree of aqueous alteration [1]. Chondrites that are a petrologic type 3, termed “unequilibrated chondrites”, lie in the middle of this scale and are therefore the least metamorphosed/ altered. Type 3 chondrites can be sub-divided into increments of 0.1 (3.0, 3.1, etc.) on the basis of their thermoluminescent properties [2], and types 3.0 through 3.2 can be sub-divided into increments of 0.05 (3.00, 3.05, etc.) based on the distribution of Cr in olivine phenocrysts [3]. Unequilibrated chondrites contain the best record of what happened in the solar nebula and protoplanetary disk, due to a lack of overprinting of parent body processes.

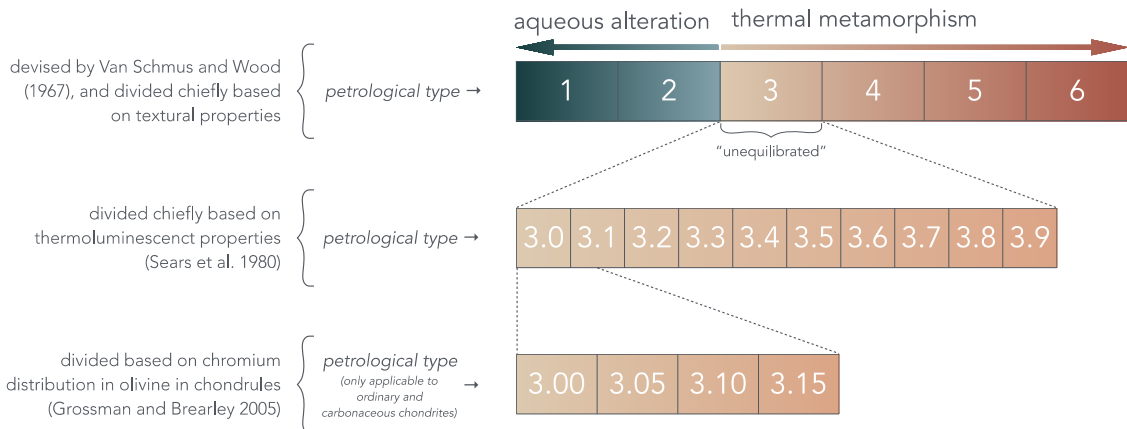


Figure 1. A petrologic type is assigned to a chondrite to indicate the amount of metamorphism or aqueous alteration it underwent on its parent asteroid.

The main two types of inclusions in chondrites are CAIs and chondrules. CAIs (Ca-Al-rich inclusions) are irregular-shaped inclusions (Fig. 2) that formed via direct condensation from the solar nebula (see for a MacPherson [4] review on CAI petrology and formation), and are rich in Ca- and Al-bearing oxides (mainly spinel and melilite). CAIs make up  $\sim 1$  vol% of chondrites, and are the earliest surviving solids to have formed in the Solar System [5, 6]. Chondrules, the dominant ( $\sim 50$  vol%) and eponymous constituent of most chondrites, are spherical ferromagnesian silicate objects (Fig. 2) that formed via flash heating and subsequent rapid cooling of precursor

dust (see Lauretta *et al.* [7]) for a review on chondrule petrology and formation). During the cooling phase of their formation, chondrules crystallised via igneous fractional crystallisation. Chondrules are mostly composed of olivine, pyroxene, and trace amounts of Fe-Ni-metal and triolite, all set in a glassy-cryptocrystalline matrix [8].

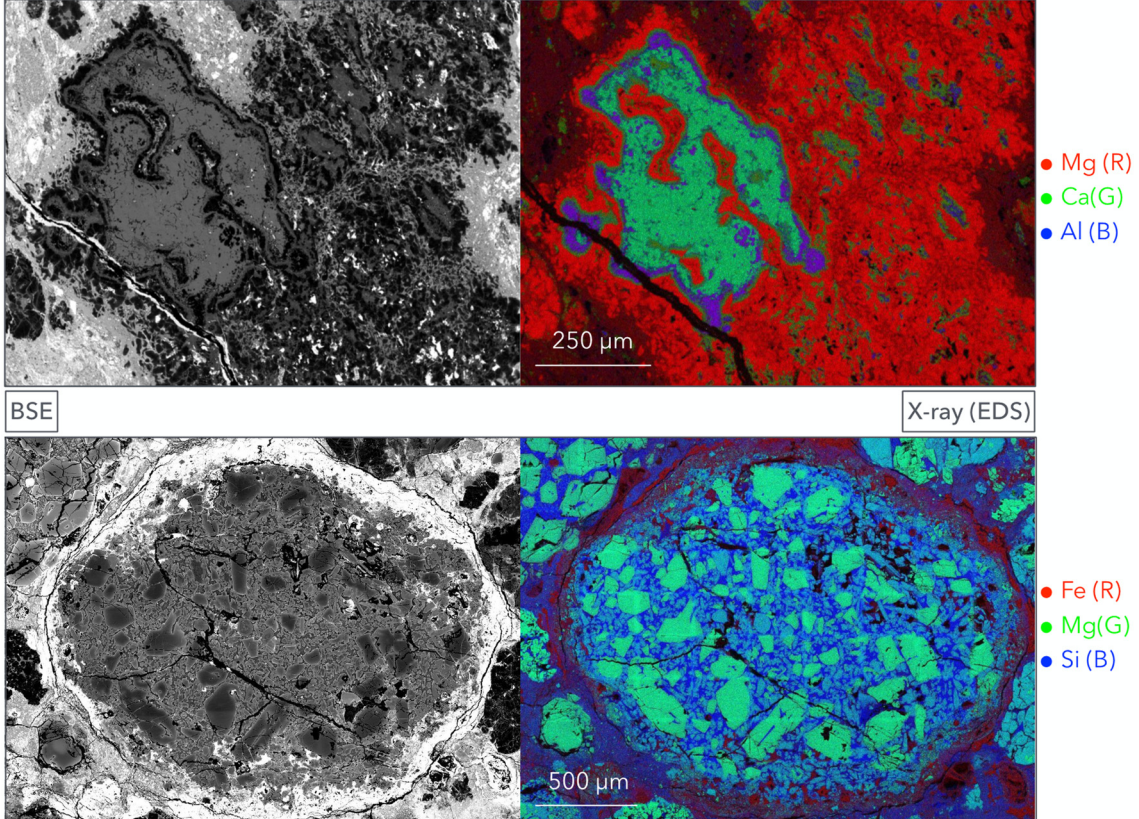


Figure 2. A CAI (top) and a chondrule (bottom), imaged in back-scattered electrons (BSE) and energy-dispersive X-ray spectroscopy (EDS). CAIs are rich in spinel and melilite, and chondrules are rich in ferromagnesian silicates (mainly olivine and pyroxene) and glassy-cryptocrystalline mesostasis.

A minor ( $\sim 0.1$  vol% [9]) and less-well studied inclusion found in chondrites are refractory forsterite (RF) grains. They are ubiquitous in unequilibrated chondrites. RFs are composed of almost pure forsterite ( $\text{Fo}_{>98}$ , where  $\text{Fo}_{\#} = \text{molar Mg}/[\text{Mg} + \text{Fe}] \times 100$ ), the Mg end-member of olivine ( $\text{Mg}_2\text{SiO}_4$ ). Compared to “normal” olivine in the same meteorite, they are enriched in the refractory lithophile elements (RLEs) Al, Ca, and Ti [10], depleted in Mn and Ni [9], and enriched in  $^{16}\text{O}$  [11]. RFs are often found in the cores of olivine phenocrysts in chondrules [12] and are in chemical and isotopic disequilibrium with the surrounding olivine; they are therefore thought to pre-date at least the chondrules in which they are found, representing part of the chondrule precursor dust. They are also found as coarse phenocrysts inside some chondrules [13] and as

isolated grains outside of chondrules [14]. Aside from the case of oxygen (e.g., Weinbruch *et al.* [11]), their isotopic composition is poorly characterised.

Chondritic inclusions, especially those from unequilibrated chondrites, contain chemical and isotopic information about the earliest few millions of years of the Solar System's history. In the case of RFs, little is known about their isotopic composition, making them novel and interesting targets for isotopic analysis. High-precision isotope analyses via inductively coupled plasma mass spectrometry (ICP-MS) is one of the most precise techniques by which the isotopic composition of these inclusions can be measured, but inevitably requires the sample to be completely destroyed. It is important that RFs are well characterised prior to destructive isotope analysis. Thorough characterisation allows isotopic analyses to be put into context, and allows links between petrology and isotopic compositions to be investigated.

Electron beam techniques are an ideal tool for non-destructive sample characterisation and identification of chondrite components of interest.

## 2. ***SAMPLE PREPARATION & ANALYSIS***

Three meteorites were chosen as part of this study: Northwest Africa (NWA) 4502 (CV3), NWA 8276 (L3.0), and Felix (CO3.3). They were chosen on the basis of their availability, and the minor amount of metamorphism that they experienced on their parent asteroids (they are all petrologic type 3).

Polished sections were made: five of NWA 4502, and five of NWA 8276. The pre-made section of Felix was borrowed from the Natural History Museum, London. Each sample was prepared using an Al-free polishing agent (a combination of SiC and diamond), since Al is an element of interest.

Each sample was carbon-coated prior to any SEM or EPM analysis. The old coat was removed using a tissue and petroleum ether and fresh coat applied around once per month to ensure the coat remained uniform and undamaged.

### 2.1. *Imaging*

Each section was imaged in backscattered electron (BSE) mode at the University of Bristol using a HITACHI S-3500N. Hundreds of individual tiles were imaged in high-magnification ( $\sim 1 \mu\text{m pixel}^{-1}$ ), and stitched together in ImageJ using the Grid/Collection Stitching plug-in [15]. Each tile was acquired at an accelerating voltage of 20 keV at a working distance of  $\sim 15$  mm, at a resolution of  $2048 \times 1536$  for 120 seconds ( $38 \mu\text{s pixel}^{-1}$ ). The high-magnification mosaics were

made primarily to serve as a way to navigate each section in subsequent work, but also as a way to preserve a record of these precious samples that will ultimately be destroyed during isotope analysis.

X-ray maps of olivine grains of interest within each section were imaged using energy-dispersive X-ray spectroscopy (EDS) on a HITACHI S-3500N at the University of Bristol. Depending on the size of the object, a magnification of between  $\times 150$  and  $\times 600$  was used. An accelerating voltage of 15 keV was used, and individual maps were acquired at either (a)  $1024 \times 768$  with a dwell time of  $76 \mu\text{s pixel}^{-1}$ , or (b)  $512 \times 384$  with a dwell time of  $305 \mu\text{s pixel}^{-1}$ , depending on the size of the grain being imaged. Each image is composed of between 120 and 1800 frames at 60 s per frame, at a working distance of  $\sim 15$  mm. X-rays maps were exported as high-resolution background-corrected net counts on Thermo Scientific NSS software, and montaged into false-colour element maps using ImageJ (Fig. 3).

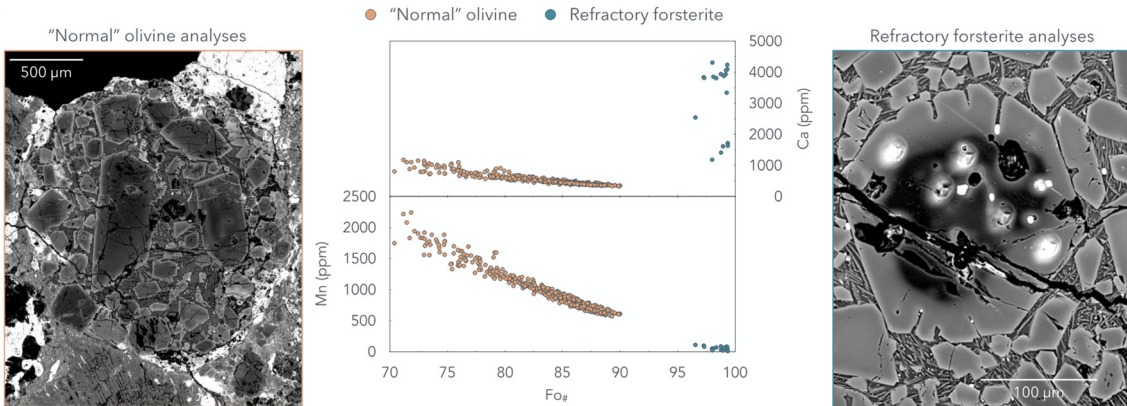


Figure 3. An example of a refractory forsterite grain (right; the dark area in the olivine) in a polished section of NWA 8276 (L3.0). The grain of interest was found using the whole-sample mosaic, then imaged using high-magnification BSE and EDS (Green = Mg, red = Ca). For comparison, a chondrule that does not contain any RFs is shown (left). Note: the ‘holes’ in the grain are pits from the secondary ionisation mass spectrometry analysis.

## 2.2. Mineral chemistry

The major (Fe, Mg, and Si) and minor (Al, Ca, Mn, Ni, and Ti) elemental compositions of olivine grains were quantitatively measured using wavelength-dispersive X-ray spectroscopy (WDS) electron probe microanalysis (EPMA) at the University of Bristol using a JEOL JXA-8530F FEG EMP Hyperprobe. An accelerating voltage of 20 keV was used throughout. Dual analytical conditions were used to maximise counting statistics and minimise the time required for each analysis: major element conditions (beam current = 20 nA, spot-size = 1  $\mu\text{m}$ ) and trace element conditions (beam current = 100 nA, spot-size = 3  $\mu\text{m}$ ). These conditions and count times are summarised in Fig. 4. Each analysis took  $\sim 5$  minutes.

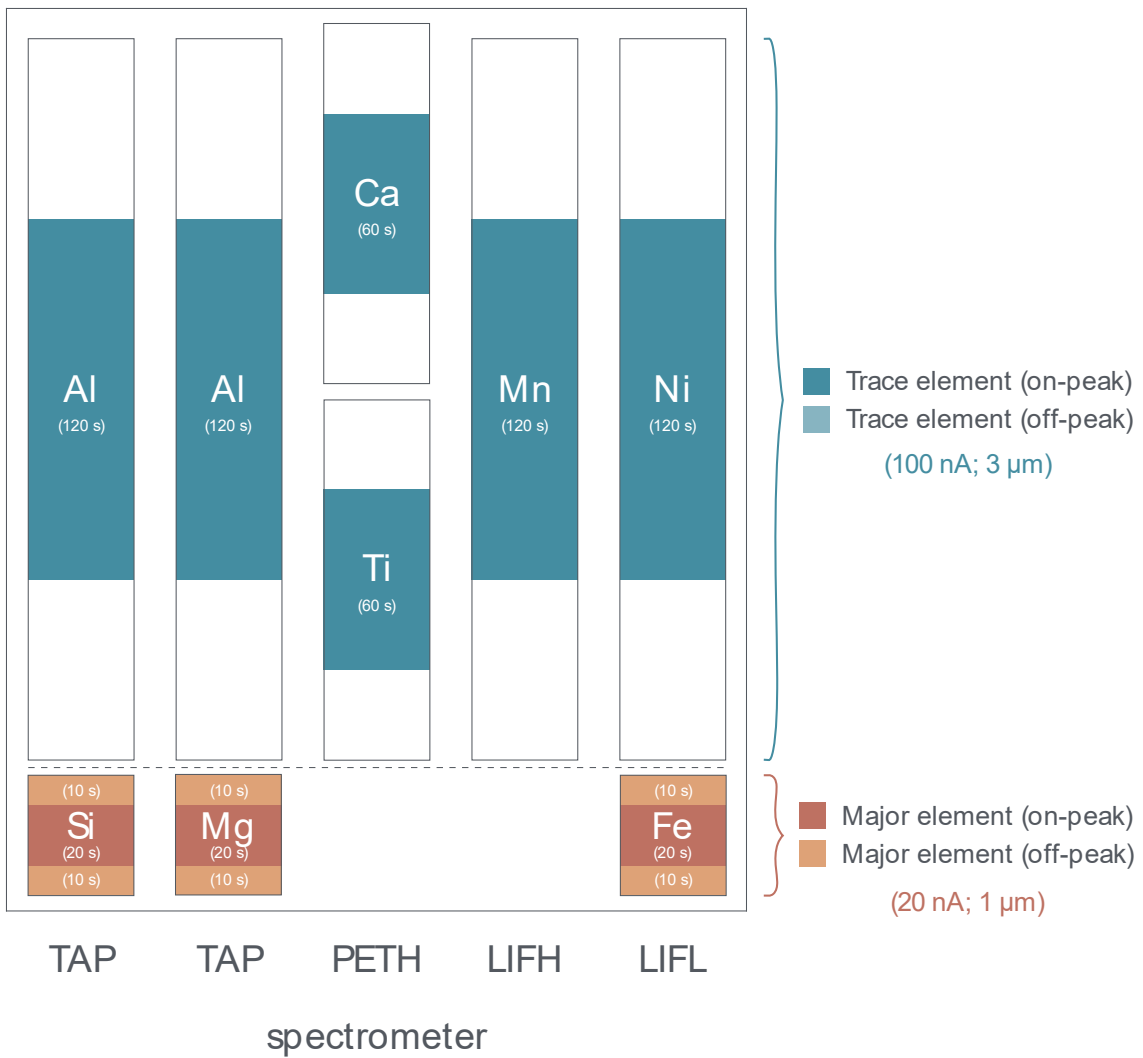


Figure 4. Dual conditions were used to measure major elements and trace elements.

The following well-characterised materials were used for calibration of each element: Al (sanidine), Ca (wollastonite), Fe (fayalite), Mg (forsterite), Mn (Mn-metal), Ni (Ni-metal), Si (forsterite), and Ti (TiO<sub>2</sub>). Instrumental drift was corrected for and applied to all measurements by re-running standards at 6-to-8-hour intervals throughout each session. Well characterised matrix-matched samples (St. John's Olivine and Navajo Olivine) were measured at the beginning and end of each session to check for accuracy and reproducibility. Stoichiometric processing was applied to all measurements, and only measurements with analytical totals of  $100 \pm 2\%$  were accepted.

### 3. RESULTS

Major and trace elements were measured to high precision, and detection limits were low enough to characterise all of the target grains. Typical uncertainties and detection limits are summarised in Table 1. Of the ~2500 individual olivine analyses made during this project, ~2100 (86 %) of them had analytical totals of  $100 \pm 2 \%$ .

Table 1. A summary of uncertainties and detection limits for each element for a given analysis.

Element	Typical uncertainty ( $2\sigma$ )	Target detection limit	Typical detection limit
Fe	0.10 wt%	-	98 ppm
Mg	0.15 wt%	-	127 ppm
Si	0.09 wt%	-	84 ppm
Al	16 ppm	~500 ppm	11 ppm
Ca	25 ppm	~1400 ppm	14 ppm
Mn	47 ppm	~100 ppm	25 ppm
Ni	29 ppm	~100 ppm	21 ppm
Ti	34 ppm	~500 ppm	26 ppm

The high-spatial resolution of the EPMA analyses ( $\sim 3 \mu\text{m}$ ) allowed even heavily fractured grains to be chemically characterised, which is advantageous for meteorites that have suffered shock and alteration on their parent asteroid.

#### 3.1. RF characterisation

Over 50 grains were selected as EPMA targets, and those which met the RF criteria ( $\text{Fo}_{\sim 98}$ , RLE-rich, and Mn- and Ni-poor) were well characterised using a combination of SEM and further EPMA (Fig. 5). X-ray EDS mapping revealed many RFs contained high-Al/Mg and high-Ca/Mg inclusions that will be properly characterised in future work. These high-Al/Mg and -Ca/Mg phases were often difficult to properly distinguish using back-scattered electron imaging.

RFs are clearly resolvable from “normal” olivine within the same meteorite (e.g., Fig. 3). They are in strong disequilibrium with surrounding/host olivine, which is a testament to the unequilibrated nature of these particular meteorites.

The high spatial resolution of EPMA allow detailed profiles to be taken across RF grain boundaries, revealing zoning in major elements and minor elements (e.g., Fig. 6).

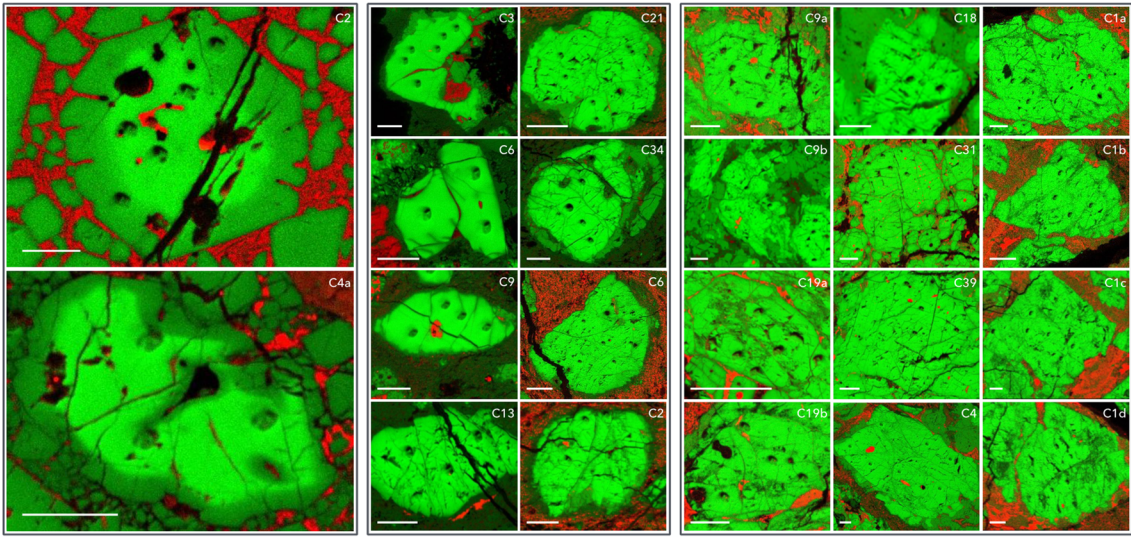


Figure 5. Twenty-one RFs across the three meteorites that have been extensively imaged using SEM, both in BSE and EDS, and characterised using EPMA. These images are EDS images (green = Mg, red = Ca). Scale bars = 50  $\mu$ m.

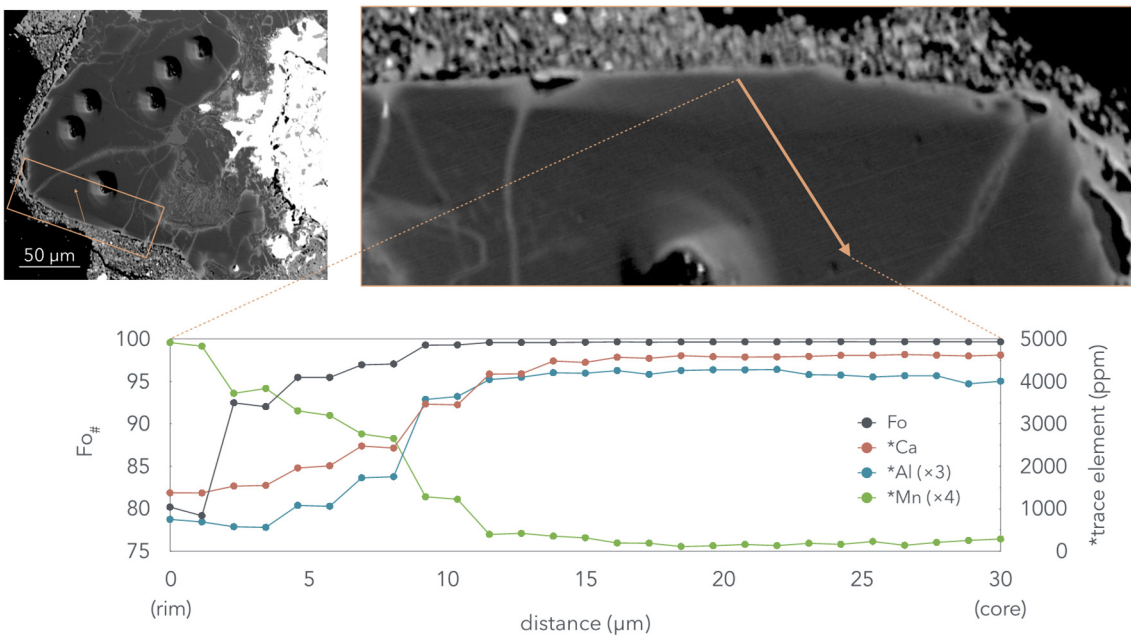


Figure 6. The zoning profile across the rim of an RF in Felix (CO3.3). Refractory lithophile elements (Al and Ca) follow the zoning profile of Mg (expressed here as Fo $\#$ ), which increase in concentration towards the core. Mn shows the inverse trend.

While other *in situ* techniques could be used to measure the trace element composition of these samples with lower detection limits and higher precision (e.g., laser ablation ICP-MS), they are destructive, and in this case lower detection limits and more precise data are not needed. The difference in trace element concentrations between “normal” olivine and RFs are orders of magnitude greater than the analytical uncertainties.

#### 4. CONCLUSIONS

Scanning electron microscopy and electron probe microanalysis provide an ideal means to characterise extraterrestrial silicate minerals. This is useful in and of itself for many applications but is particularly useful prior to destructive analysis such as mass spectrometry. The high spatial resolution ( $\sim 3 \mu\text{m}$  scale) and the low detection limits (down to tens of ppm for some elements) of EPMA allow thorough chemical characterisation of grains, and high-magnification SEM imagery using multiple SEM signals (e.g., BSE, EDS) allow for their petrographic context to be well understood.

In this project, I have taken over 5,000 SEM images and made over 2,000 good (analytical total  $100 \pm 2 \%$ ) electron probe analyses. BSE and EDS imagery on an SEM is routine and unchallenging for silicate minerals. Once an analysis protocol has been established on the electron probe and checked against secondary standards, this technique is also routine. High-quality data from both instruments can be acquired with relative ease.

Importantly, these techniques allow destructive measurements such as isotope analyses to be put into context, and allow a record of precious extraterrestrial samples to be archived post-destruction.

#### 5. ACKOWLEGEMENTS

A huge thank you to Ben Buse and Stuart Kearns for the help and assistance when using the SEM and electron probe at the University of Bristol, and the Natural History Museum (London) for the section of Felix. This work was funded by my PhD funding body, NERC, through the NERC GW4+ DTP.

#### 6. REFERENCES

- [ 1] Van Schmus W R and Wood J A 1967 A chemical-petrologic classification for the chondritic meteorites. *Geochim. Cosmochim. Acta* **31** 747-765
- [ 2] Sears D W, Grossman J N, Melcher C L, Ross L M and Mills A A 1980 Measuring metamorphic history of unequilibrated ordinary chondrites. *Nature* **287** 791-795
- [ 3] Grossman J N and Bearley A J 2005 The onset of metamorphism in ordinary and carbonaceous chondrites. *Meteorit. Planet. Sci.* **40** 87-122
- [ 4] MacPherson G J 2014 in: *Treatise on geochemistry*. (New York, NY: Elsevier) 139-179
- [ 5] Amelin Y, *et al.* 2010 U-Pb chronology of the Solar System's oldest solids with variable  $^{238}\text{U}/^{235}\text{U}$ . *Earth Planet. Sci. Lett.* **300** 343-350
- [ 6] Brennecke G A, Budde G and Kleine T 2015 Uranium isotopic composition and absolute ages of Allende chondrules. *Meteorit. Planet. Sci.* **50** 1995-2002

- [ 7] Lauretta D S, Nagahara H and Alexander C M O 2006 in: *Meteorites and the early Solar System II*. (Lauretta D S and McSween H Y; Eds.) (Tucson, AZ: University of Arizona Press) *The University of Arizona space science series*, 431-459
- [ 8] Jones R H 1996 FeO-rich, porphyritic pyroxene chondrules in unequilibrated ordinary chondrites. *Geochim. Cosmochim. Acta* **60** 3115-3138
- [ 9] Pack A, Yurimoto H and Palme H 2004 Petrographic and oxygen-isotopic study of refractory forsterites from R-chondrite Dar al Gani 013 (R3.5-6), unequilibrated ordinary and carbonaceous chondrites. *Geochim. Cosmochim. Acta* **68** 1135-1157
- [10] Steele I M, Smith J V and Skirius C 1985 Cathodoluminescence zoning and minor elements in forsterites from the Murchison (C2) and Allende (C3V) carbonaceous chondrites. *Nature* **313** 294-297
- [11] Weinbruch S, Zinner E K, El Goresy A, Steele I M and Palme H 1993 Oxygen isotopic composition of individual olivine grains from the Allende meteorite. *Geochim. Cosmochim. Acta* **57** 2649-2661
- [12] Steele I M 1989 Compositions of isolated forsterites in Ornans (C3O). *Geochim. Cosmochim. Acta* **53** 2069-2079
- [13] Jones R H and Scott E R D 1989 in: *19th Lunar and Planetary Science Conference* (Houston, TX) 523-536
- [14] Fuchs L H, Olsen E and Jensen K J 1973 Mineralogy, mineral-chemistry, and composition of the Murchison (C2) meteorite. *Smithson. Contrib. Earth Sci.* **10** (available at <http://repository.si.edu/handle/10088/804>
- [15] Preibisch S, Saalfeld S and Tomancak P 2009 Globally optimal stitching of tiled 3D microscopic image acquisitions. *Bioinformatics* **25** 1463-1465